Modeling of Pile Stabilized Clay Slopes using a Large Deformation Finite-Element Method

Ripon Karmaker & Bipul Hawlader
Department of Civil Engineering, Faculty of Engineering and Applied Science
Memorial University of Newfoundland, St. John's, NL, Canada

ABSTRACT

Slope stabilization using passive piles is an effective and popular solution for both onshore and nearshore environments. The limit equilibrium (LE) method is commonly used for stability analysis of slopes. However, this method of analysis cannot calculate the stress and deformation of a pile–soil system properly. Finite-element (FE) method could be used to overcome some of these limitations. The present study uses a Coupled Eulerian–Lagrangian approach to model pile stabilized clay slopes for undrained loading conditions. The strength reduction method is used to trigger the failure of the slope. The progressive formation of failure planes, large deformation of the failed soil mass and flow of soil between the piles are examined. The increase in factor of safety by a row of piles at the middle of the slope is presented.

RÉSUMÉ

La stabilisation des pentes à l'aide de pieux passifs est une solution efficace et populaire pour les environnements onshore et nearshore. La méthode de l'équilibre limite (LE) est couramment utilisée pour l'analyse de la stabilité des pentes. Cependant, cette méthode d'analyse ne peut pas calculer correctement la contrainte et la déformation d'un système pile-sol. La méthode des éléments finis (FE) pourrait être utilisée pour surmonter certaines de ces limitations. La présente étude utilise une approche couplée eulérienne-lagrangienne pour modéliser des pentes d'argile stabilisées sur pieux pour des conditions de chargement non drainé. La méthode de réduction de la force est utilisée pour déclencher la défaillance de la pente. La formation progressive de plans de rupture, la grande déformation de la masse de sol défaillante et l'écoulement du sol entre les pieux sont examinés. L'augmentation du facteur de sécurité par une rangée de pieux au milieu de la pente est présentée.

1. INTRODUCTION

Piles are used to stabilize marginally stable slopes in onshore and nearshore environments. Unlike typical laterally loaded pile foundations, where the lateral load comes to the pile head and then transfer to the soil (active piles), the piles used for slope stabilization are considered as passive piles because the lateral load comes from soil displacements. In the design of piles for slope stabilization, two key questions are: (i) for a given configuration (pile spacing, size and location), how much factor of safety will be increased by the piles; and (ii) how much soil load will come to the piles, which is required to calculate the length and diameter and selection of pile type. In the current design practice, the following three steps are followed: (i) calculate the additional resistive force required to achieve the desired factor of safety (F_s), (ii) estimate the resisting force a pile can provide to resist the movement of the soil mass above the potential failure plane, and (iii) select appropriate type and size of the pile and also the location along the slope.

Proper estimation of force on the pile is difficult because it is resulted from a complex process of soil displacement and even squeezing through the space between the piles. Empirical, analytical and numerical techniques have been used to estimate the lateral force on a pile. Among them, the modulus of subgrade reaction method (e.g., Chow 1996; Ashour et al. 1998; Kourloulis et al. 2012) is a very simple one for industry practice. However, appropriate judgement is required to estimate this parameter. For clays, the ultimate resistance per metre length of a single lateral loaded pile (p_u) can be related to the undrained shear strength of clay (s_u) as $p_u = N.s_uD$, where D is the diameter of the pile and N is constant which could vary between 9 and 12 (Matlock 1970) and also could vary with depth (Poulos 1995). Ito and Matsui (1975) proposed a theoretical solution to calculate the lateral force acting on rigid slope stabilizing piles that could squeeze the soil between the piles.

Numerical techniques, such as finite element and finite difference, have also been used for improved pile–soil interaction modeling. Rowe and Poulos (1979) conducted finite-element analysis to investigate undrained pile–soil interaction with an idealized plane strain condition of the three-dimensional problem. Oakland and Chameau (1986) conducted elastic finite-element analysis for pile stabilized surcharged slopes. Kourkoulis et al. (2012) proposed a hybrid method for analysis and design of slope stabilizing piles. They decoupled the problem and calculated the lateral force on the pile by conducting finite-element simulation where an upper soil block slides along a predefined horizontal slip surface over a stable soil block. In addition, boundary-element method has been used to calculate the increase in F_s and to develop simplified methods for analysis and design of pile stabilized slopes.

The above FE modeling has been conducted using Lagrangian-based finite-element methods. It has been also recognized that when soil strength is low and/or pile spacing is large, soil might squeeze or flow through the space between the piles. In such cases, large deformation of soil occurs. The objective of the present study is to simulate pile–soil interaction using a Coupled Eulerian–Lagrangian (CEL) approach that allows simulation of large deformation. The performance of pile stabilized slopes with two clay layers of varying geotechnical properties is investigated.

2. PROBLEM DEFINITION

A 10-m high slope (2H : 1V) of two clay layers is analyzed in this study (Fig. 1). The analysis is performed for undrained loading condition. The slope is marginally stable and a row of vertical piles (D = 0.8 m) is installed at the middle of the slope to increase the factor of safety. The pile in installed sufficiently large depth below the clay layer. However, the simulation is performed only for the clay domain, assuming the pile as a rigid body. The authors understand that the flexibility of the pile have some influence on factor of safety (F_s), which is one of the limitations of this study.

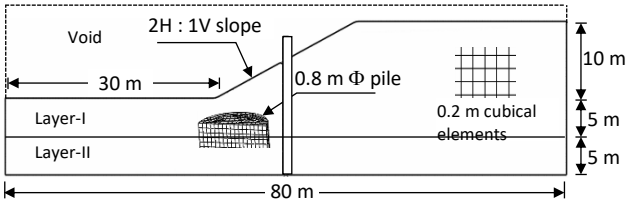

Figure 1. Pile stabilized slope used in FE modeling

3. FINITE-ELEMENT MODELING

The Coupled Eulerian–Lagrangian (CEL) approach in Abaqus 6.14-2 FE software is used for numerical analysis. The soil is modeled as an Eulerian material such that it can displace large distance without causing any numerical issues related to mesh distortion. The pile is modeled as a rigid Lagrangian body and extended up to the bottom of the domain. The pile is also extended 2 m above the slope such that the effects of accumulated soil in the right side of the pile after the failure of the slope can be modeled.

Three-dimensional finite-element analysis is performed with the thickness of the domain in the out-of-plane direction in Fig. 1 of s/2, where s is the centre-to-centre spacing between the piles. The model consists of three parts: soil, pile and a void space above the soil to accommodate displaced soil. To develop the model, an Eulerian domain is first created, which is then filled with soil using the Eulerian Volume Fraction (EVF) tool in Abaqus. For an element, EVF = 1 means that the element is filled with soil and EVF = 0 represents the void elements.

Soil is modeled using the EC3D8R elements in Abaqus, which are 8-node linear multi-material Eulerian brick element. The pile is discretized first using C3D8R elements, which are 8-node linear brick elements, and then defined as a rigid body.

The left and right boundaries are placed sufficiently far from the slope and pile, in order to avoid boundary effects. Zero velocity boundary conditions are applied normal to all the vertical faces of domain shown in Fig. 1. At the bottom of the domain, zero velocity boundary conditions are applied in all three directions (i.e., $v_x = v_y = v_z = 0$). No boundary condition is applied along the soil–void interface. An unbonded rough pile–soil interface condition, which is based on a general contact algorithm, is used.

Mesh sensitivity analysis is carried out and an optimum mesh size of 0.2 m × 0.2 m × 0.2 m is obtained. The soil is modeled as an elastic–perfectly plastic material using the undrained shear strength (s_u). The yield strength, which is an input parameter in Abaqus, is calculated as $\sqrt{3}s_u$. The finite-element modeling consists of two loading steps. Firstly, the gravitational loading is applied by increasing the gravitational acceleration to bring the soil to in-situ stress condition by maintaining the ratio between horizontal and vertical total stress equal to 1.0. It is understood that the earth pressure at rest could have a significant effect on slope failure. However, in this study the effect of at-rest earth pressure coefficient is not investigated. In the second step, s_u is slowly reduced with time to maintain quasi-static condition. During the reduction of s_u, the ratio between initial shear strength ($s_{u(in)}$) and reduced shear strength (s_u) at a time step is maintained the same for both clay layers (Layer-I & -II, Fig. 1), and this ratio is called the "strength reduction factor, SRF." The SRF is equivalent to F_s in typical slope stability analysis using limit equilibrium methods.

The geotechnical properties used in FE analysis are shown in Table 1. Analyses are performed for pile spacing s = 2.0–5.0.

Table 1. Geotechnical properties used in FE analysis

Soil properties	Case-A		Case-B	
	Layer I	Layer II	Layer I	Layer II
Unit weight, γ (kN/m^3)	17	19	19	17
Undrained shear strength, s_u (kPa)	30	60	60	30
Undrained Young's modulus E_u (kPa)	10,000	10,000	10,000	10,000
Undrained Poisson's ratio, ν_u	0.495	0.495	0.495	0.495

4. RESULTS

The formation of failure planes with and without piles, the deformation of soil including the arching and squeezing between two piles, and the variation of load on the pile with displacement of the failed soil block are the key factors in the design of slope stabilizing pile. In the present study, the former two are investigated.

4.1 Comparison of FE and limit equilibrium analyses

Figure 2 shows the development of plastic shear strain for Case-A soil parameters without piles. At SRF = 1.18, a large curved plastic shear zone develops causing downslope movement of the soil above this, as observed from instantaneous velocity vectors. The same slope is analyzed using the SLOPE/W software that has been developed based on limit equilibrium (LE) methods, and F_s = 1.18 is calculated. The location of the critical slip circle obtained from SLOPE/W analysis is shown by the dashed line in Fig. 2(a). This indicates the success of CEL for slope stability analysis.

SLOPE/W analysis does not provide any information about the deformation of the failed soil mass, which can be obtained from FE analysis. As shown in Fig. 2(b) that large plastic shear strains generate in a narrow zone at SRF = 1.63, together with a considerable movement of the failed soil, from where the location of the failure plane in FE analysis could be better identified.

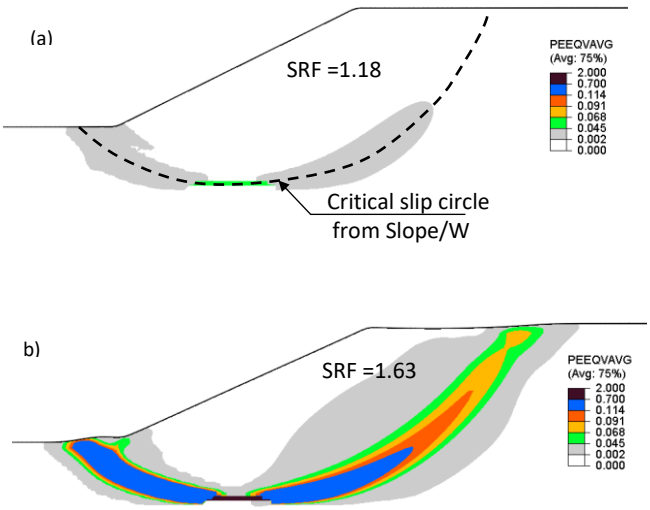

Fig 2. Comparison between FE simulation and limit equilibrium analysis results without piles

4.2 Simulation results for Case-A with pile spacing 3D

Figures 3(a–d) show the formation of shear bands with increase in SRF. At the end of geostatic step with initial $s_{u(in)}$ (i.e., SRF = 1.0), plastic shear strain does not generate in the soil. For SRF = 1.74, two shear bands form: one from the toe of the slope and the other one from the pile at the interface between the two clay layers (point A) (Fig. 3(a)). Both of them propagates towards the upslope areas. With further increase in SRF, two shear bands, originated from the interface between two soil layers, propagate in the upslope and downslope directions (Fig. 3(b) & 3(c)). The propagation of these shear bands continues with increase in SRF and the shear bands reach the ground surface, generating large plastic shear strains in these bands (Fig. 3(c)). The accumulation of shear strain continues along the previously developed shear band even at large SRF (e.g., SRF = 2.45 in Fig. 3(e)). The failed soil mass displaces significantly and a gap between the pile and displaced soil is formed behind the pile (in the left side) (Fig. 3(e)). Note that the pile–soil interface is modeled as unbonded (no-tension) condition. Moreover, the location of the global failure plane does not change, although a number of shear bands form locally in the failed soil mass, especially in the left side of the pile (Fig. 3(e)).

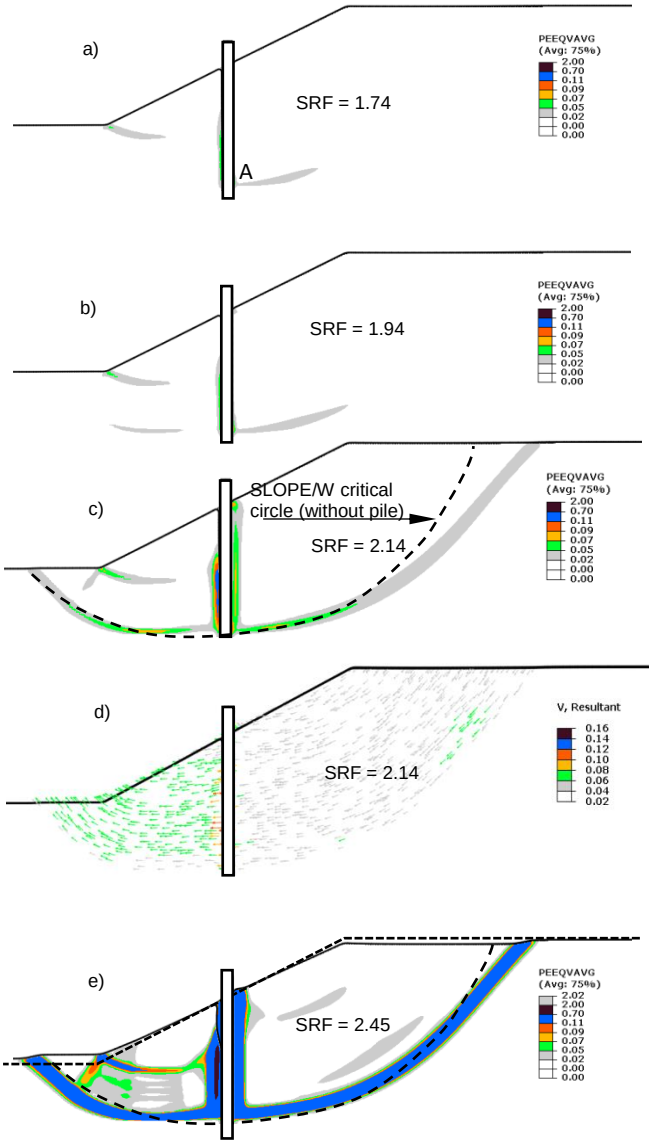

Fig. 3. Formation and propagation of failure planes for 3D pile spacing with Case-A soil parameters

The location of global failure plane is important in the design of pile stabilized slopes. In the current design practice, the increase in factor of safety is obtained from the additional resistance offered by the pile on the soil above the global failure plane (e.g. see Kourkoulis et al. 2012 for further discussion). Previous finite-element analysis considered the location of the maximum shear force in a flexible pile as the point where the critical slip

plane intersects the pile. However, Wei and Cheng (2009) found that the location of the maximum shear force in the pile does not always represent the location of the critical slip circle. They also suggested that the critical slip surface should be identified from accumulated plastic shear strain.

In finite-element slope stability analysis, different approaches have been used to identify the initiation of failure (i.e., the value of SRF that could be considered as F_s in limit equilibrium analysis). Among them, the following three criteria are commonly used: (i) formation of a band of plastic shear strain that could be considered as a global failure plane (e.g., Matsui and San, 1992), (ii) sudden nodal displacement in the mesh (e.g., Zienkiewicz et al. 1975; Griffiths and Lane 1999, Tan and Sarma 2008), and (iii) non-convergence of the solution (Zienkiewicz et al. 1975; Tan and Sarma 2008). As shown in Fig. 3 that the failure initiates locally and then propagates gradually to form a global failure plane. Therefore, the displacement of the point that can be considered to define the failure should be carefully selected, depending upon the problem. The last criterion (non-convergence) might simply be a numerical issue, especially at large displacements in typical Lagrangian-based finite-element analysis. The numerical issues could be significant when piles are used to stabilize the soil because of ill-conditioning of stiffness matrix and high stress gradient in typical Lagrangian FE models (Cai and Ugai 2000). Day and Potts (1994) suggested to use small elements near the interface between soil and structure to reduce this type of numerical issue.

The present CEL analysis does not have any numerical issue related to mesh distortion. Therefore, the solution does not stop after partial formation of failure plane due to significant mesh distortion. The mesh remains fixed and the Eulerian material (soil) flows through the mesh.

In the present study, the first criteria (i.e., formation of shear band) is used to define the failure. The location of the failure plane could be better identified from the clear shear band of high plastic shear strain, as shown in Fig. 3(e). Note that, such a large deformation generally cannot be simulated using typical Lagrangian FE programs.

For comparison, the location of the critical circle obtained from SLOPE/W without pile is shown by a dashed line in Figs. 3(c) and 3(e). The global failure plane obtained from FE analysis with pile is slightly outside the critical slip circle obtained from SLOPE/W analysis without pile, for this case. However, the global failure plane intersects the pile at the same depth—the interface between two clay layers—in both analyses (i.e., FE and LE). It is to be noted here that, for a c–ϕ soil, Wei and Cheng (2009) showed shallower failure planes in the pile stabilized slope than in the same slope without pile.

4.3 Effects of pile spacing

Figures 4(a–d) show the plastic shear strains in the soil in four vertical planes starting from the centre of the pile (z = 0) to the half way between two adjacent piles ($z = s/2$) for SRF = 1.67. Here, z represents the coordinate in the out-of-plane direction, measured from the centre of the pile. Figure 4(a) shows that plastic shear strains generate not only in the global failure plane but also in the both sides of the pile. During the downslope movement of the failed soil block, soil elements move around the pile, as shown in the inset of Fig. 4(a), which generates plastic shear strain around the pile. The magnitude of plastic shear strain decreases with z—highest on the plane that passes through the centre of the pile (i.e., z = 0, Fig. 4(a)) and the lowest at $z = s/2$ (Fig. 4(d)).

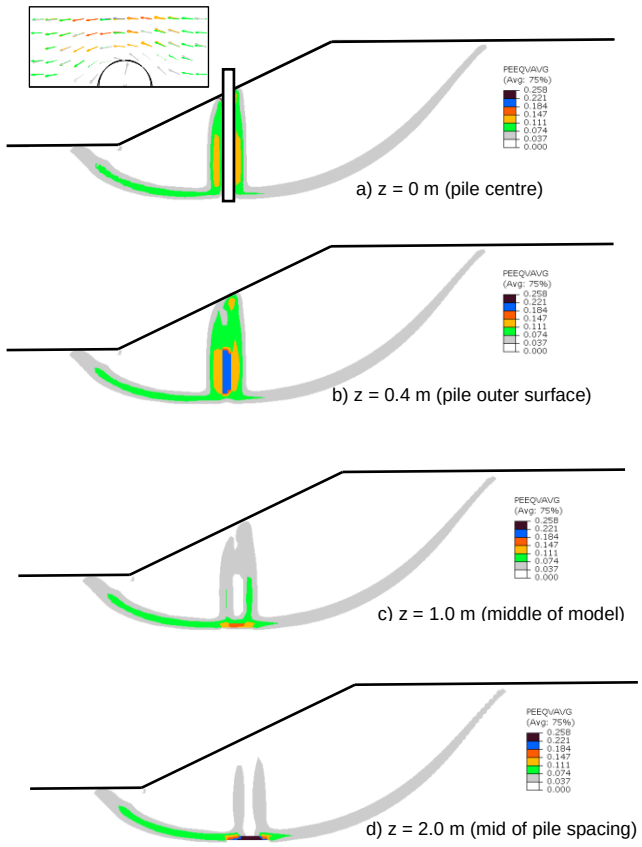

Fig. 4. Effect of pile on strain development in soil (Case-A)

4.4 Simulation results for Case-B with pile spacing 3D

Figures 5(a–c) show the formation of failure planes with increase in SRF for the Case-B soil parameters. As the weaker clay layer is below the stronger clay, a deep seated global failure plane originating from the base of the weak layer is obtained. A complete global failure plane generates at a large SRF in this case as compared to Case-A (compare Figs. 3(c) and 5(c)). Moreover, the formation of local shear bands in the failed soil mass in this case is also different from Case-A, as shown in Fig. 3. Figure 5(d) shows the instantaneous velocity vectors for SRF = 2.41. The F_s of this slope without pile is ~ 1.36, as obtained from SLOPE/W and FE analyses.

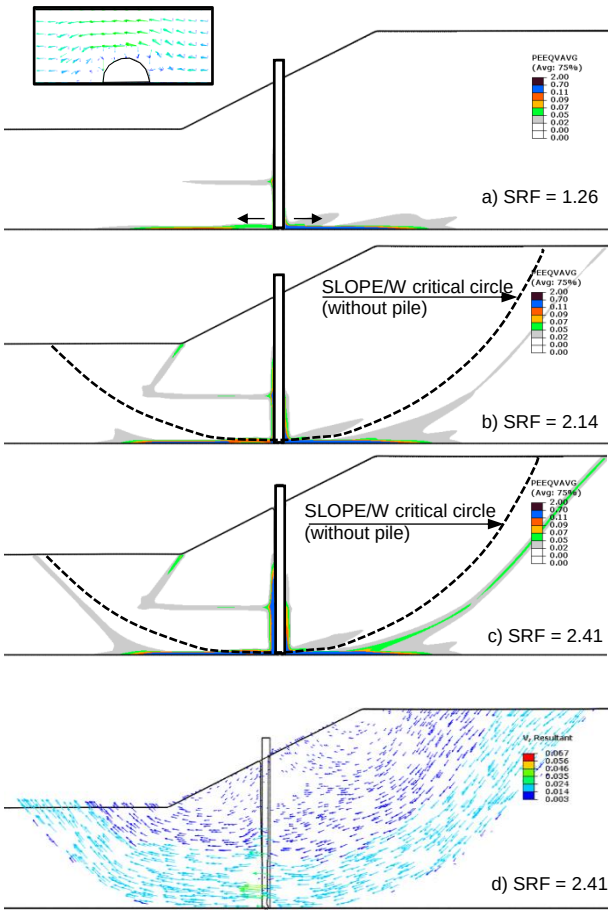

Fig. 5. Formation and propagation of failure planes for 3D pile spacing with Case-B soil parameters

4.5 Increase in factor of safety

The success of using piles for slope stabilization is generally checked by the increase in factor of safety. Figure 6 shows the stability improvement ratio, $N_{ps} = F_{ps}/F_s$, with pile spacing for the two cases analyzed in the present study. Here, F_{ps} is the factor of safety for pile stabilized slope, F_s is the factor of safety without pile. Also, F_{ps} represents the value of SRF at which a global failure plane develops in FE analysis, as discussed above. To calculate N_{sp}, the value of F_s obtained from FE results is used, which is also similar to the value of F_s in limit equilibrium analysis. Figure 6 shows that a row of pile could significantly increase the F_s—for example, at s = 3, the F_s is increased by ~ 80%. Moreover, N_{ps} decreases with increasing pile spacing; however, even at s = 5, the piles could increase the F_s by 40% of the F_s without piles. It is to be noted here that, for a c–ϕ soil, Wei and Cheng (2009) found the effect of pile on F_s is negligible after s = 10–14.

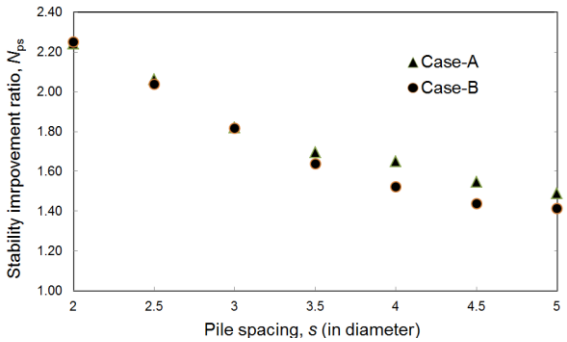

Fig. 6: Effects of pile spacing on increase in factor of safety

5. CONCLUSIONS

Finite element analysis of pile-reinforced clay slopes is presented in this paper. The slope has two layers of clay, which has been modeled using the undrained shear strength of soil. The numerical modeling is performed using the Coupled Eulerian-Lagrangian approach in Abaqus FE software, where the soil is modeled as an Eulerian material and pile as a Lagrangian body. The following conclusions can be drawn from this study:

a) The global failure plane passes through the bottom of the weaker clay layer in both conditions (overlain or underlain by a strong layer).
b) The existence of piles slightly increases the size of the failure wedge, as compared to that of the slope without pile; however, the depth of the failure plane at the pile location (mid-slope) is the same.
c) For the cases analyzed, the factor of safety increases even for centre-to-centre spacing of 5.

Finally, although the present analyses show the success of CEL approach for modeling pile–slope interaction, even for large deformations, it has some limitations. The analyses have been performed using rigid piles installed at the mid-slope. Further studies considering the flexibility of the pile for different locations along the slope need to be investigated

6. ACKNOWLEDGEMENTS

The research works presented in this paper have been funded by MITACS and NSERC.

7. REFERENCES

ABAQUS 6.14 [Computer software]. D. S. Simulia, *Dassault Systémes*.

Ashour, M., Norris, G.M. and Pilling, P. 1998. Lateral loading of a pile in layered soil using the strain wedge model, *Journal of Geotechnical and Geoenvironmental Engineering*, 124(4): 303–315.

Cai, F. and Ugai, K. 2000. Numerical analysis of the stability of a slope reinforced with piles, *Soils and Foundations*, 40(1): 73–84.

Chow, Y.K. 1996. Analysis of piles used for slope stabilization, *International Journal for Numerical and Analytical Methods in Geomechanics*, 20(9): 635–646.

Day, R.A. and Potts, D.M. 1994. Zero thickness interface elements-numerical stability and application, *International Journal for Numerical and Analytical Methods in Geomechanics*, 18(10): 689-708.

Griffiths, D. V. and Lane, P. A. 1999. Slope stability analysis by finite elements, *Géotechnique*, 49(3): 387–403.

Ito, T. and Matsui, T. 1975. Methods to estimate lateral force acting on stabilizing piles, *Soils and Foundations*, 15(4): 43–59.

Kourkoulis, R., Gelagoti, F., Anastasopoulos, I. and Gazetas, G. 2012. Hybrid method for analysis and design of slope stabilizing piles, *Journal of Geotechnical and Geoenvironmental Engineering*, 137(1): 1–14.

Matlock, H. 1970. Correlation for design of laterally loaded piles in soft clays, *2nd Annual Offshore Technology Conference*, Houston, Texas, 1: 577–588.

Matsui, T. and San, K. 1992. Finite element slope stability analysis by shear strength reduction technique, *Soils and Foundations*, 32(1): 59–70.

Oakland, M.W. and Chameau, J. 1986. *Drilled pilers used for slope stabilization*, Joint Highway Research Project, Indiana Department of Transportation and Purdue University, West Lafayette, Indiana, FHWA/IN/JHRP-86/07.

Poulos, H.G. 1995. Design of reinforcing piles to increase slope stability, *Canadian Geotechnical Journal*, 32(5): 808–818.

Rowe, R.K. and Poulos, H.G. 1979. A method for predicting the effect of piles on slope behaviour, 3rd *International Conference on Numerical Methods in Geomechanics*, Achen, 3: 1073–1085.

SLOPE/W 2018, 4th ed., *GEO- SLOPE International Ltd.*, Calgary, AB, Canada.

Tan, D. and Sarma, S.K. 2008. Finite element verification of an enhanced limit equilibrium method for slope analysis, *Géotechnique*, 58(6): 481–487.

Wei, W.B. and Cheng, Y.M. 2009. Strength reduction analysis for slope reinforced with one row of pile, *Computers and Geotechnics*, 36: 1176–1185.

Zienkiewicz, O.C., Humpheson, C. and Lewis, R.W. 1975. Associated and non-associated viscoplasticity and plasticity in soil mechanics. *Géotechnique*, 25(4): 671–689.